

AD-A096 031

RENSSELAER POLYTECHNIC INST TROY N Y F/G 13/8
THE RELATIONSHIP OF STRUCTURE AND PROPERTIES TO DEPOSITION COND--ETC(U)
FEB 81 R J DIEFENDORF, J L BENJAMIN DAAG29-77-G-0167

ARO-14380.1-MS

NL

UNCLASSIFIED

1 1
ADA
500 241

END
GPO
FPM:EF
A-81
DTIC

UNCLASSIFIED

SECURITY CLASSIFICATION OF THIS PAGE (When Data Entered)

REPORT DOCUMENTATION PAGE

READ INSTRUCTIONS
BEFORE COMPLETING FORM

1. REPORT NUMBER 14380.1-MS	2. GOVT ACCESSION NO. AD-A096 031	3. RECIPIENT'S CATALOG NUMBER
4. TITLE (and Subtitle) The Relationship of Structure and Properties to Deposition Conditions and the Origin of Residual Stress in CVD Silicon Carbide and Nitride		5. TYPE OF REPORT & PERIOD COVERED Final Report 10 Jun 77 - 31 Dec 79
7. AUTHOR(s) R. J. Diefendorf J. L. Benjamin W. A. Hargreaves		8. CONTRACT OR GRANT NUMBER(s) DAAG29-77 G 0167
9. PERFORMING ORGANIZATION NAME AND ADDRESS Rensselaer Polytechnic Institute Troy, NY 12181		10. PROGRAM ELEMENT, PROJECT, TASK AREA & WORK UNIT NUMBERS
11. CONTROLLING OFFICE NAME AND ADDRESS U. S. Army Research Office Post Office Box 12211 Research Triangle Park, NC 27709		12. REPORT DATE Feb 13, 1981
14. MONITORING AGENCY NAME & ADDRESS (if different from Controlling Office)		13. NUMBER OF PAGES 55
		15. SECURITY CLASS. (of this report) Unclassified
		15a. DECLASSIFICATION/DOWNGRADING SCHEDULE
16. DISTRIBUTION STATEMENT (of this Report) Approved for public release; distribution unlimited.		
17. DISTRIBUTION STATEMENT (of the abstract entered in Block 20, if different from Report) NA		
18. SUPPLEMENTARY NOTES The view, opinions, and/or findings contained in this report are those of the author(s) and should not be construed as an official Department of the Army position, policy, or decision, unless so designated by other documentation.		
19. KEY WORDS (Continue on reverse side if necessary and identify by block number) silicon carbide chemical vapor deposition residual stress structural materials crystallographic structures hydrogen deposition		
20. ABSTRACT (Continue on reverse side if necessary and identify by block number) Two limiting factors in the acceptance of CVD SiC as a structural material have been deposition control and residual stress in the deposit. Deposition parameters have been related to morphological as well as crystallographic structures. The effect of various additions to the basic methyltrichlorosilane and hydrogen deposition gases has also been studied and the effect on structure noted. Deposition rate control through the interaction of these parameters has also been obtained. Residual stresses large enough to crack deposits have been observed. Although no		

DTIC
ELECTE
MAR 6 1981

UNCLASSIFIED

SECURITY CLASSIFICATION OF THIS PAGE (When Data Entered)

AD A 096031

DRG FILE COPY

20. ABSTRACT CONTINUED

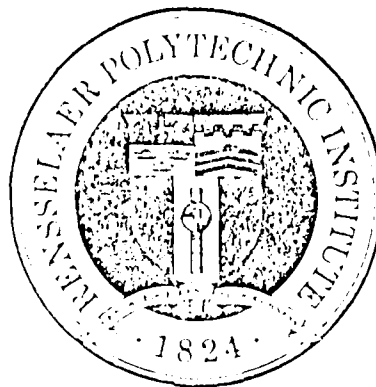
quantitative model has been determined to predict these stresses, a qualitative model has been proposed which allows the trends in residual stress to be predicted. This model is based on structure. Finally, the strength of CVD SiC was determined using a biaxial tensile test to obtain a closer approximation of the as-deposited strength than is possible with three or four-point bend tests.

Acquisition For	
W. D. ORAM	
1. 1981	
2. 1982	
3. 1983	
4. 1984	
5. 1985	
6. 1986	
7. 1987	
8. 1988	
9. 1989	
10. 1990	
11. 1991	
12. 1992	
13. 1993	
14. 1994	
15. 1995	
16. 1996	
17. 1997	
18. 1998	
19. 1999	
20. 2000	
21. 2001	
22. 2002	
23. 2003	
24. 2004	
25. 2005	
26. 2006	
27. 2007	
28. 2008	
29. 2009	
30. 2010	
31. 2011	
32. 2012	
33. 2013	
34. 2014	
35. 2015	
36. 2016	
37. 2017	
38. 2018	
39. 2019	
40. 2020	
41. 2021	
42. 2022	
43. 2023	
44. 2024	
45. 2025	
46. 2026	
47. 2027	
48. 2028	
49. 2029	
50. 2030	
51. 2031	
52. 2032	
53. 2033	
54. 2034	
55. 2035	
56. 2036	
57. 2037	
58. 2038	
59. 2039	
60. 2040	
61. 2041	
62. 2042	
63. 2043	
64. 2044	
65. 2045	
66. 2046	
67. 2047	
68. 2048	
69. 2049	
70. 2050	
71. 2051	
72. 2052	
73. 2053	
74. 2054	
75. 2055	
76. 2056	
77. 2057	
78. 2058	
79. 2059	
80. 2060	
81. 2061	
82. 2062	
83. 2063	
84. 2064	
85. 2065	
86. 2066	
87. 2067	
88. 2068	
89. 2069	
90. 2070	
91. 2071	
92. 2072	
93. 2073	
94. 2074	
95. 2075	
96. 2076	
97. 2077	
98. 2078	
99. 2079	
100. 2080	
101. 2081	
102. 2082	
103. 2083	
104. 2084	
105. 2085	
106. 2086	
107. 2087	
108. 2088	
109. 2089	
110. 2090	
111. 2091	
112. 2092	
113. 2093	
114. 2094	
115. 2095	
116. 2096	
117. 2097	
118. 2098	
119. 2099	
120. 2100	
121. 2101	
122. 2102	
123. 2103	
124. 2104	
125. 2105	
126. 2106	
127. 2107	
128. 2108	
129. 2109	
130. 2110	
131. 2111	
132. 2112	
133. 2113	
134. 2114	
135. 2115	
136. 2116	
137. 2117	
138. 2118	
139. 2119	
140. 2120	
141. 2121	
142. 2122	
143. 2123	
144. 2124	
145. 2125	
146. 2126	
147. 2127	
148. 2128	
149. 2129	
150. 2130	
151. 2131	
152. 2132	
153. 2133	
154. 2134	
155. 2135	
156. 2136	
157. 2137	
158. 2138	
159. 2139	
160. 2140	
161. 2141	
162. 2142	
163. 2143	
164. 2144	
165. 2145	
166. 2146	
167. 2147	
168. 2148	
169. 2149	
170. 2150	
171. 2151	
172. 2152	
173. 2153	
174. 2154	
175. 2155	
176. 2156	
177. 2157	
178. 2158	
179. 2159	
180. 2160	
181. 2161	
182. 2162	
183. 2163	
184. 2164	
185. 2165	
186. 2166	
187. 2167	
188. 2168	
189. 2169	
190. 2170	
191. 2171	
192. 2172	
193. 2173	
194. 2174	
195. 2175	
196. 2176	
197. 2177	
198. 2178	
199. 2179	
200. 2180	
201. 2181	
202. 2182	
203. 2183	
204. 2184	
205. 2185	
206. 2186	
207. 2187	
208. 2188	
209. 2189	
210. 2190	
211. 2191	
212. 2192	
213. 2193	
214. 2194	
215. 2195	
216. 2196	
217. 2197	
218. 2198	
219. 2199	
220. 2200	
221. 2201	
222. 2202	
223. 2203	
224. 2204	
225. 2205	
226. 2206	
227. 2207	
228. 2208	
229. 2209	
230. 2210	
231. 2211	
232. 2212	
233. 2213	
234. 2214	
235. 2215	
236. 2216	
237. 2217	
238. 2218	
239. 2219	
240. 2220	
241. 2221	
242. 2222	
243. 2223	
244. 2224	
245. 2225	
246. 2226	
247. 2227	
248. 2228	
249. 2229	
250. 2230	
251. 2231	
252. 2232	
253. 2233	
254. 2234	
255. 2235	
256. 2236	
257. 2237	
258. 2238	
259. 2239	
260. 2240	
261. 2241	
262. 2242	
263. 2243	
264. 2244	
265. 2245	
266. 2246	
267. 2247	
268. 2248	
269. 2249	
270. 2250	
271. 2251	
272. 2252	
273. 2253	
274. 2254	
275. 2255	
276. 2256	
277. 2257	
278. 2258	
279. 2259	
280. 2260	
281. 2261	
282. 2262	
283. 2263	
284. 2264	
285. 2265	
286. 2266	
287. 2267	
288. 2268	
289. 2269	
290. 2270	
291. 2271	
292. 2272	
293. 2273	
294. 2274	
295. 2275	
296. 2276	
297. 2277	
298. 2278	
299. 2279	
300. 2280	
301. 2281	
302. 2282	
303. 2283	
304. 2284	
305. 2285	
306. 2286	
307. 2287	
308. 2288	
309. 2289	
310. 2290	
311. 2291	
312. 2292	
313. 2293	
314. 2294	
315. 2295	
316. 2296	
317. 2297	
318. 2298	
319. 2299	
320. 2300	
321. 2301	
322. 2302	
323. 2303	
324. 2304	
325. 2305	
326. 2306	
327. 2307	
328. 2308	
329. 2309	
330. 2310	
331. 2311	
332. 2312	
333. 2313	
334. 2314	
335. 2315	
336. 2316	
337. 2317	
338. 2318	
339. 2319	
340. 2320	
341. 2321	
342. 2322	
343. 2323	
344. 2324	
345. 2325	
346. 2326	
347. 2327	
348. 2328	
349. 2329	
350. 2330	
351. 2331	
352. 2332	
353. 2333	
354. 2334	
355. 2335	
356. 2336	
357. 2337	
358. 2338	
359. 2339	
360. 2340	
361. 2341	
362. 2342	
363. 2343	
364. 2344	
365. 2345	
366. 2346	
367. 2347	
368. 2348	
369. 2349	
370. 2350	
371. 2351	
372. 2352	
373. 2353	
374. 2354	
375. 2355	
376. 2356	
377. 2357	
378. 2358	
379. 2359	
380. 2360	
381. 2361	
382. 2362	
383. 2363	
384. 2364	
385. 2365	
386. 2366	
387. 2367	
388. 2368	
389. 2369	
390. 2370	
391. 2371	
392. 2372	
393. 2373	
394. 2374	
395. 2375	
396. 2376	
397. 2377	
398. 2378	
399. 2379	
400. 2380	
401. 2381	
402. 2382	
403. 2383	
404. 2384	
405. 2385	
406. 2386	
407. 2387	
408. 2388	
409. 2389	
410. 2390	
411. 2391	
412. 2392	
413. 2393	
414. 2394	
415. 2395	
416. 2396	
417. 2397	
418. 2398	
419. 2399	
420. 2400	
421. 2401	
422. 2402	
423. 2403	
424. 2404	
425. 2405	
426. 2406	
427. 2407	
428. 2408	
429. 2409	
430. 2410	
431. 2411	
432. 2412	
433. 2413	
434. 2414	
435. 2415	
436. 2416	
437. 2417	
438. 2418	
439. 2419	
440. 2420	
441. 2421	
442. 2422	
443. 2423	
444. 2424	
445. 2425	
446. 2426	
447. 2427	
448. 2428	
449. 2429	

FINAL TECHNICAL REPORT

GRANT No. DAAG29-77-G-0167

THE RELATIONSHIP OF STRUCTURE AND PROPERTIES
TO DEPOSITION CONDITIONS AND THE ORIGIN OF RESIDUAL
STRESS IN CVD SILICON CARBIDE AND NITRIDE



R. J. DIEFENDORF
(PRINCIPAL INVESTIGATOR)

J. L. BENJAMIN

W. A. MAGEE

FEBRUARY 13, 1981

81 2 2 072

ABSTRACT

Two limiting factors in the acceptance of CVD SiC as a structural material have been deposition control and residual stress in the deposit. Deposition parameters have been related to morphological as well as crystallographic structures. The effect of various additions to the basic methyltrichlorosilane and hydrogen deposition gases has also been studied and the effect on structure noted. Deposition rate control through the interaction of these parameters has also been obtained. Residual stresses large enough to crack deposits have been observed. Although no quantitative model has been determined to predict these stresses, a qualitative model has been proposed which allows the trends in residual stress to be predicted. This model is based on structure. Finally, the strength of CVD SiC was determined using a biaxial tensile test to obtain a closer approximation of the as-deposited strength than is possible with three or four-point bend tests.

INTRODUCTION

Silicon carbide is a candidate material for high-temperature sections of energy conversion devices. Its attractiveness results from a combination of high strength at elevated temperatures, high modulus, good thermal conductivity, relatively low thermal expansion and excellent oxidation resistance to temperatures of 1600°C. Since high structural integrity is necessary for such devices, materials forming options are needed which do not introduce strength-reducing flaws. These include chemical vapor deposition (CVD), hot-pressing, and sintering. CVD is under study since high purity, theoretically dense, controlled microstructure material may be deposited directly to the desired form. Sintering and hot-pressing require the addition of sintering aids which decrease high-temperature properties. Machining, with the resultant strength-reducing flaws, is also often not required with CVD materials. Gulden¹ has measured the strength of very small pieces of silicon carbide (.040" wide x .004" thick x .062" outer gauge length) using 4-pt. bend tests. He found the strength to be relatively constant from room temperature to 940°C and in the range of from 106,000 to 144,000 psi. A general increase to the range from 134,000 to 189,000 psi was observed as temperature was increased to 1400°C. For CVD SiC deposited at R.P.I., Weiss² has reported an average room temperature strength of 48,000 to 72,000 psi for larger specimens. Testing to 1400°C increased the average strength to 80,000 psi, while testing at 1500°C resulted in a 180,000 psi average strength. Breaking at room temperature after heating to 1400°C in air resulted in increasing room temperature strength to 80,000 psi. These values demonstrate the excellent high temperature strength possible with CVD SiC. Creep was not measureable at 1550°C, an applied load of 50,000 psi, and a machine sensitivity of better than 10^{-9} per second.

DIRECTION OF WORK

Given these advantages, what limiting factors prevent the use of CVD SiC? Cost has been traditionally high, primarily because little scientific knowledge has been used to determine the best set of deposition parameters to form the material with the desired structure and deposition profile. In addition, stresses are developed in the deposits which range from several thousand psi, which reduce the useful strength of the deposit, to those causing fracture of the material. These fractures have been observed both during deposition and upon cool-down of the system. These two areas are the primary targets for this research.

DEPOSITION CONTROL

Chemical vapor deposition is a molecular forming process where a gas or gases containing the desired deposit atoms are passed over a heated substrate and form the desired material. The reaction is in general endothermic. CVD as a process is theoretically less well understood than physical vapor deposition where fundamental variables such as supersaturation may be more definitely specified. However, certain concepts relevant to any nucleation and growth process are still valid. The number of nucleation sites should increase as the supersaturation of the system increases. The analysis of this step for a CVD system is more complex, however, as more than one species is in general participating in the deposition process which makes a simple definition of supersaturation difficult. Also, substrates are in general less than perfect, and surface defects and impurities which act as nucleation sites are very prevalent. Chemical reaction of the depositing species to form the nucleus also complicates nucleation calculations. Figure 1 illustrates the difficulties. Shown are the first-deposited surface of two specimens deposited under nominally

equal conditions. Very different nucleation densities have resulted, but whether they are from substrate differences or initial fluctuations in growth conditions is not clear.

Growth from these nuclei is controlled by several processes, any of which can be rate-limiting. For the CVD of SiC, (1) the methyltrichlorosilane (MTCS) must be decomposed in the region adjacent to the substrate, (2) the resulting reactive species must be transported to the substrate surface, (3) these species must be adsorbed and then diffuse and react, (4) product species must be then desorbed and finally transported away. MTCS is the precursor most commonly used in the CVD of SiC because of its relative ease of handling, availability, and one to one carbon to silicon ratio. Figure 2 illustrates schematically the steps in the growth process for the formation of SiC from MTCS. Maximum deposition rate will be achieved when mass transport is the controlling step (high reactant flux), while uniform deposition over an extended substrate is best achieved when surface kinetics are controlling (generally low temperature).

Thermodynamic calculations can determine the equilibrium gas phase composition. However, due to changing temperature and concentration profiles as the gas flows in the tube, it must be kept in mind that these are only the best thermodynamic estimate as to the actual species present. Using the free energy minimization technique as outlined by Oliver³ for the determination of equilibrium gas phase composition, the predominant gas phase species were determined to be C_2H_2 , $SiCl_2$, H_2 , and HCl for typical deposition conditions used here at R.P.I. The fact that $SiCl_2$ is the predominant silicon containing species is important in that its presence is one of the reasons why hydrogen has been found necessary for

the deposition of pure SiC. Thermally decomposing MTCS alone or with an inert gas gives rise to severe nucleation problems as well as the deposition of free graphite. This was determined initially by Popper⁴ and since confirmed by many researchers. Cartwright¹¹ has theorized a decomposition of MTCS as shown in Figure 3. He notes that the carbon-silicon bond is the weakest in the compound, and therefore the first to break as the molecule is heated. SiCl_2 , a stable molecule, is theorized to be the silicon reactive species. Excess hydrogen is required to reduce this molecule so that silicon is available for the deposition of SiC. Excess hydrogen also inhibits the decomposition of methyl radicals which would result in excess carbon or pyrolytic graphite deposition. Since carbon and silicon are depositing independently, an input ratio of one carbon to one silicon atom is not sufficient to insure the deposition of stoichiometric silicon carbide. The ability of the gas phase to absorb excess silicon or carbon by the formation of silicon chlorides or methyl radicals which are thermodynamically stable in the vapor phase will also inhibit excess carbon or silicon deposition.^{5A}

Various additions to the system have been examined at R.P.I. Silicon tetrachloride was used in an attempt to improve high temperature deposits. At higher temperatures, silicon incorporation into the deposit becomes increasingly difficult as its relative supersaturation decreases. Though the maximum deposition rate decreased somewhat, where excess carbon or poor nucleation had been a problem, the deposits obtained with the SiCl_4 addition were good silicon carbide. The addition of HCl to inhibit excess silicon deposition at low temperatures by forming gas phase silicon chlorides was also attempted. Large amounts of HCl at 1350°C completely halted deposition while smaller amounts led to the formation of closely spaced islands of SiC. These results indicate

that the gas phase composition for the production of good SiC is very close to that currently being used ($H_2:MTCS \approx 2:1$).

Acetylene and methane were added to study their effect on composition as well as structure. It was hoped that a continuously nucleated material could be produced with excess carbon in the system so that the typical growth cone structure could be avoided. This was not successful. At the upper temperature limit where good SiC is formed, an acetylene addition resulted in pyrolytic graphite formation with only a few scattered islands of SiC. Lower temperatures produced a powdery deposit. A methane addition gave a very smooth deposit compared to one without methane, but growth cones still extended through the thickness of the deposit.

The particular furnace system used at R.P.I. is schematically shown in Figure 4. It consists of a resistance heated graphite which radiantly heats the graphite substrate through which the reactive gas mixture is fed through. Gas flow is controlled by rotameters or mass flow controllers. The entire system is operated at reduced pressure (typically five to ten mm Hg) to avoid gas phase nucleation from high supersaturation. This is the alternative to operating at atmospheric pressure where an inert diluent gas such as argon must be added. Temperature is measured by an optical pyrometer. The system design is what is known as a "hot-wall reactor". The other option is the "cold-wall reactor" where the gas is passed by a resistance heated rod or wire. This introduces large thermal and concentration gradients in the gas which are eliminated in the "hot-wall" configuration. The gas temperature and concentration of reacting species both reach steady-state values after an initial period during which the gas is being heated to deposition temperature and reactive

species formed. Further down the tube the concentration of reactant decreases as it is stripped by deposition. These idealized profiles are illustrated in Figure 5 which also shows the resulting characteristic deposition profile.

The effect of varying deposition parameters on both structure and deposition profile has also been analyzed. Weiss² has measured deposition profiles as single parameters were varied. As an example Figure 6 shows that increasing deposition temperature shifts the maximum in deposition rate towards the inlet. Increasing the flow rate flattens the deposition profile as does higher initial concentrations of MTCS. The use of other reactants will also have an effect on the deposition profile as illustrated in Figure 7 where methyldichlorosilane has been substituted for MTCS. Here the shift in deposition maximum is due to less chlorine in the system allowing silicon to be incorporated in the deposit as opposed to various gas-phase silicon chloride compounds.

Knowledge and control of the resulting microstructure is also important. A scanning electron microscopy study of morphological features for various deposition parameters was undertaken. The surface morphology can be interpreted in terms of how the deposit is forming. The effect of temperature is shown in Figure 8. At 1000X, the crystal features of the high temperature deposit cover the entire field of the photograph while the lower temperature deposit has features orders of magnitude smaller. This difference is due to the decreased surface mobility of atoms during deposition at the lower temperatures.

The effect of gas phase composition can be seen in Figure 9. At 1000X, a deposit formed with 33% reactant vs. 11% is much less crystalline as surface rearrangement time is decreased at the resultant higher deposition rates.

Finally, the effect of pressure is seen in Figure 10 at 50X where at higher pressures the material exhibits deeper crevices between growth nodules. The sharper concentration gradient at higher pressure causes any protuberance to grow into the richer gas stream away from the deposit surface. This is also an indication that the growth of SiC in this system is at least partially diffusion rate limited.

Crystallographically, SiC is polytypic. This is a special form of polymorphism, where though the structure is the same in two dimensions, it varies in the third. Silicon carbide is formed by the close-packing of tetrahedrally coordinated, predominantly covalently bonded layers of silicon and carbon. The strong directional bonding is responsible for the high hardness, melting point and strength of pure SiC. Verma and Krishna⁵ have written a book discussing polytypism with an extensive review on the theories relating to SiC. Knippenberg⁶ studied both the growth and structure of SiC extensively, though primarily in its single crystal form. Any structure can be specified by stating the position of the close-packed planes; either A, B, or C just as in close-packed metals. However, one close-packed layer actually represents two combined atom layers, one silicon and one carbon. The cubic stacking sequence, ABCABC, is the β form of SiC while all other non-cubic forms are termed α . Approximately one hundred non-cubic forms have been identified, with repeating stacking sequences ranging from two to several hundred.⁷ The observation that these long period polytypes exist can be roughly understood from the fact that, as nearest-neighbor interactions are the same for all polytypes, the total energy to a first approximation does not depend on stacking order. However, no one has yet been able to formulate a comprehensive predictive theory for polytype formation. Pure polytypes are

exceedingly difficult to grow. Sato⁸ has determined the stacking order in CVD SiC to be nearly random in the direction perpendicular to the close-packed planes.

Through analysis of x-ray diffractometer scans the relative amounts of cubic and non-cubic material as a function of temperature have been determined at R.P.I. as shown in Figure 11. The minimum amount of non-cubic material probably represents for this system the closest set of conditions for which pure cubic SiC can be formed. At temperatures above this, true non-cubic material is probably formed in accordance with the general trend to non-cubic SiC at high temperatures. At lower temperatures, the non-cubic material is probably disordered silicon carbide, there not being sufficient thermal energy for the atoms to reach the lowest energy state which appears to tend toward cubic material.

RESIDUAL STRESS

The motivation for the study of residual stress in CVD SiC comes from the resultant degradation of mechanical properties of the deposit, during or after completion of deposition. Stresses in CVD SiC are not an isolated case, they occur in nearly all atomically deposited materials with resultant degradation of optical, chemical, electrical, magnetic and mechanical properties. These stresses vary from near zero to high enough to cause fracture, spalling, or delamination of the deposit. Residual stresses in electrodeposits and thin films have been explained and characterized to a certain degree, but there is still no all inclusive theory which explains all observations. CVD systems with the exception of pyrolytic graphite, which is not typical because of its high anisotropy, have been even more poorly characterized. Experimental evidence, possible mechanisms, and what is believed to be the most applicable to CVD SiC will be discussed

in this section of the report.

Residual stresses have been noted by several researchers in CVD SiC. Weiss² studied the phenomena for a range of parameters and concluded a surface tension and crystallite boundary theory best explained his experimental evidence. He also found that increases in residual stress correlated best with increases in deposition rate.

Airey⁹ characterized CVD SiC deposited on the outside of a thin, slit, graphite tube. Compressive stresses were developed which after an initial thin layer (70 microns) reached a relatively constant value. As soon as deposition was halted, further narrowing of the slit was not observed. This indicates stresses are developed during deposition and are not a result of cool-down. Lloyd¹⁰ found for deposition on large tubes, no consistent pattern of residual stress sign for either internal or external deposits. Cartwright¹¹ for deposition on heated rods again found no single sign for stresses developed, though he associated high H_2 :MTCS ratios with compressive stresses and high flow rates with tensile stresses in the coating. Crane¹² found the outer surface of SiC deposited on tungsten fibers to be in a slight tensile state. Gebhardt¹⁵ found compressive residual stresses in internal CVD Si_3N_4 deposits. He correlated greater stresses with longer gas residence times. Engdahl¹⁴ for CVD SiC formed at 1/3 atmospheric pressure found residual stress to have no relation with structure, but seemingly with impurities in the gas phase. Kamins¹⁵ observed deformation during deposition of polycrystalline silicon. It was sporadic in nature, seemingly not an intrinsic material property. He related stresses to oxygen impurities inhibiting surface diffusion.

Possible explanations for stress in CVD SiC follow. The residual stress of interest is intrinsic, not simply a mismatch between either

the thermal expansion coefficient or lattice parameter of the substrate and deposit. Evidence for this is the observed popping off of deposits during a run as well as the bowing at temperature of a deposit to which excess silicon had been added. Thus, growth type stresses are predicted to be the primary contributor to residual stress in CVD SiC.

Thermal stresses, however, are a possible explanation. These would arise from the last deposited surface being at a lower temperature than the first deposited surface, either from cooling by the reactant gas which may not have reached deposition temperature or by cooling from the endothermic deposition reaction. Though no observable difference in temperature has been measured, it may still exist over a very few atomic layers. Upon cool-down, this would put the last deposited surface in compression and the first deposited surface in tension.

An excess energy theory detailed by Hoar and Arrowsmith¹⁶ explains the origin of stresses with a model of surface atoms having a higher energy than the bulk. This would be of little importance in thick deposits, and as pointed out by Powell¹⁷ is probably more applicable to deposits formed by methods other than CVD such as sputtering where the impinging atoms have a much greater energy.

Phase changes and the resultant volume change would also introduce stress. As outlined, SiC has polytypic structure related to undefined deposition variables. Using Gomes-De Mesquita's crystallographic data, the difference in volume between the two most extreme structures would be less than 0.1%.¹⁸ This would not produce stresses of the magnitude necessary to fracture the material as has been observed. It may, however, vary the magnitude of observed stresses as different variables result in varying amounts of cubic material.

Hydrogen stresses are important in many systems, especially electro-deposits. Hydrogen is used in the deposition process in large quantities. However, the lowest stresses are found when the highest ratio of hydrogen is used, though the structure is radically different. Causey¹⁹ has determined the solubility of deuterium at 1200°C in SiC and found it to be approximately 4×10^{-4} deuterium per silicon atom and decreasing with increasing temperature. This implies the amount of hydrogen in deposits is very small.

Diffusion stresses would include elimination of lattice dislocations, vacancies, or other defects from a deposit. Klokholm and Berry²⁰ theorized such an effect for evaporated metal films. The growth layer would not be fully dense if atoms did not have sufficient time to diffuse to equilibrium positions prior to being buried by the atomic layer of the deposit. Subsequent annealing to a denser structure will introduce tensile stresses in the deposit. The very low creep rate found for CVD SiC as well as its high melting or dissociation temperature indicate that atomic mobility within the deposit is quite limited at deposition temperature. As pointed out by Kamins¹⁵, a possible mechanism leading to a decreased mobility of the depositing atoms would be incorporation of impurity atoms such as oxygen into the growth front. This would lead to a less ordered structure than would be possible in the absence of the impurity.

As detailed by Powell¹⁷, anisotropy may also lead to stresses. In amorphous or polycrystalline material, local stresses have small magnitudes and tend to cancel out due to random structure. However, CVD materials tend to deposit with a definite preferred orientation, leading to a "growth anisotropy" preventing neutralization of local stresses. Other features which would introduce anisotropy would include any systematic variation in crystal size, material composition, or density of lattice vacancies,

inclusions, or dislocations. The large anisotropy of pyrolytic graphite in conjunction with actual growth of the deposit during deposition is one of the extreme examples of this phenomena leading to large residual stresses. Baratta²¹ has derived equations for stresses arising on cool-down of an anisotropic material in cylindrical form. For typical deposition conditions and geometries used here at R.P.I., a compressive stress of approximately 4,000 psi is calculated for the first deposited surface. Though this may add a constant value to determined room temperature stresses, it is not large enough to account for observed values.

A defect theory has been proposed by Popereka²² for electrodeposits. Since all deposited layers are formed under similar conditions, usually with a pronounced growth direction, dislocations of one sign will predominate in crystals of a deposit. If dislocations were free to move, the repulsion of similar dislocations would cause them to move to surfaces and disappear causing a reduction in volume in the deposit and resultant tensile stress. Though CVD SiC deposits atomically as do electrodeposits, dislocations do not easily move, nor has there been a high density of dislocations observed.²³

Hoar and Arrowsmith¹⁶ combined this mechanism with various surface effects to explain stresses in electrodeposits. If excess vacancies exist at the surface, a situation as shown in Figure 12a would develop leading to a tensile stress in the material. If impurities were adsorbed on the surface as shown in Figure 12b, compressive stresses would result.

The model Weiss proposed² for CVD SiC was a combined surface tension and crystallite boundary mismatch one. There are several possibilities of how surface tension can contribute to residual stress. The first is that proposed by Hoar and Arrowsmith.¹⁶ They theorized that for rapidly deposited electrodeposits, equilibrium would not be reached and each layer after being buried by the next depositing layer may retain some of the

surface tension associated with a solid surface. As detailed by Powell,¹⁷ there is also the possibility of a "quasi-liquid" phase existing at high temperatures in CVD deposits. This model is tentative at best due to the lack of knowledge of the stress state of liquids at high temperature and still less of solids at any temperature.

Stress from surface tension in a more conventional sense as shown by Chopra²⁴ would be:

$$\text{Stress} = \frac{\sigma_1 + \sigma_2}{t}$$

where σ_1 is the surface tension of the deposit-gas interface, σ_2 is the surface tension of the deposit-substrate interface, and t is the thickness of the film. This would be important only for much thinner deposits than are presently under observation.

Several researchers have formulated surface tension effects with crystallite mismatch effects^{25,26} for electrodeposits. This is basically what Weiss has proposed for CVD SiC². An initial compression is set up due to surface tension of the discrete nuclei. As the nuclei become bonded to the substrate and grow laterally, tension is developed from attraction as well as the tendency to reduce surface area at grain boundaries. As Weil²⁵ points out, as grain size increases, stress should decrease due to less grain boundary area. However, larger grains also tend to have a higher degree of boundary mismatch leading to greater tensile stresses. What would therefore be expected is a tensile stress increasing to a continuous value as the deposit becomes continuous. Weiss² theorized a compressive stress in the first deposited surface due to surface tension of individual grains. As competitive growth proceeds between crystallites such as growth cone interfaces, further compressive stresses were theorized to develop. This compressive stress would decrease

as the growth cones became increasingly parallel. Powell¹⁷ points out that surface tension or tension due to lattice vacancies and dislocations between cone shaped aggregates will have a horizontal component varying as the cosine of a normal to the substrate and the side of the growth cone. The magnitude will be greater on the substrate side due to smaller grains, but the cosine of the angle may be smaller at this point. Therefore, stresses from surface tension will reach a maximum close to, but not necessarily at the substrate interface.

Experimentally, residual stresses have been measured in several ways at R.P.I. A flat deposit was analyzed through its thickness for stress determination by analysis of the bending resulting from material removal on the last-deposited surface. The results are shown in Figure 13. As can be seen, a high compressive stress was found at the first deposited surface, consistent with the decreasing radius of curvature as material was removed. This is also consistent with the experimental observation that when tube-like deposits are slit in the longitudinal axis, the outside radius in general shows a decrease in dimension. However, very thick coarsely nucleated deposits formed upon flat plates have shown a tendency to have the first deposited surface in tension. Experimental evidence for this is open cracks at the first deposited surface of such deposits formed here at R.P.I.

While these statements may appear contradictory, Lloyd¹⁰ also found inconsistency in the sign of the residual stresses in his deposits of SiC, though no explanation was offered. What appears to be occurring is that in addition to the stresses resulting from surface tension and crystallite mismatch, stresses arise from the competitive growth of the cone-like features of the deposit. The growth component parallel to the substrate

is inhibited by competing growth cones. However, since the reaction is at least partially diffusion rate limited growth cones exhibiting preferred growth directions will crowd out others. Finely nucleated deposits, as are generally formed in the 1" I.D. tubes used for most of the deposits at R.P.I., would be expected to have large compressive stresses at the first deposited surface followed by compressive stresses of decreasing magnitude. The final profile would show the first deposited surface in compression and the last in tension. Coarsely nucleated structure would show little stress at the first deposited surface followed by increasing compressive stress as the growth cones began to crowd each other out. The final stress profile would show the first deposited surface in tension with the last in compression. (See Figure 13A.)

Some experimental evidence for this is seen in Figure 14. The $\{111\}$ preferred orientation can be thought of as a measure of orientation of these growth cones as the $\langle 111 \rangle$ direction is the preferred direction of CVD SiC. This finely nucleated structure took several mils to reach a nearly constant preferred orientation. Thus, a compressive stress at the first deposited surface would be expected. This is consistent with the fact that only in coarsely deposited material have tensile cracks appeared at the first deposited surface.

Additional evidence for this mechanism can be seen in Figure 15. This is a poorly nucleated sample, but what is important to notice is the spherical shape of the deposit which did form. In a deposit which nucleated evenly, as the nuclei attempted to gain this spherical shape, they would be inhibited by impingement with other nuclei. This would set up compressive stresses.

This is also consistent with the observation by Weiss² that residual stress levels correlated best with deposition rate. These high deposition

rates also tend to fine nucleation. Though his explanation is probably mechanically correct, it is not a true surface tension and crystallite boundary mismatch explanation. It would be better termed the preferential or competitive growth mechanism.

Using strain gauges as shown below, stress was measured in one-inch diameter tubes of material, approximately 200 mils thick. The most rapidly deposited material tested (1500°C , $\text{H}_2/\text{MTCS} = 2:1$; 6 CFH H_2) showed the highest residual stress, nearly 80,000 psi. The test configuration is shown in Figure 16.

Finally, using a biaxial test rig as shown in Figure 17, the strength of several pieces of silicon carbide prepared at R.P.I. was measured. This test rig was patterned after the one proposed by Wachtman.²⁷ It was thought that this type of measurement would provide a better feeling for the intrinsic value of strength of CVD SiC, as only a highly polished surface is subjected to the maximum tensile stress. This is different than three or four-point bend tests where the edges of the test samples often suffer from machining damage. Prior to testing, the samples were given a vacuum anneal at 1400°C for 15 minutes. The motivation for this heat-treatment was similar to that of Johnson,²⁸ that is to blunt surface cracks. In our experiment, it was not thought necessary to remove several μm of material, however. The goal was to blunt flaws that were nearly of an atomic level. Since the samples had taken several weeks to prepare, drastic annealing was deemed undesirable. The four specimens yielded strengths of 54, 74, 81 and 118 Kpsi. These samples were 1.1 inches in diameter and 50 mils thick. Several conclusions were made at the time using the Weibull modulus calculated. Although four samples is indeed a small sample size. However,

the most important conclusion which can be drawn from these results is that using the Weibull modulus calculated from previous tests of CVD SiC at R.P.I. as well as the volume of these samples—the predicted biaxial strength would have been 59,000 psi. The values obtained indicate that if CVD SiC can be formed directly to shape, eliminating the need for machining, higher strengths can be expected than predicted by bend tests.

CONCLUSIONS

(1) While varying deposition geometries will yield different results, the best results using MTCS and H_2 as the reactant gas will be obtained near 1450°C and a 2:1 MTCS/ H_2 ratio. If the resultant deposit raises from the desired structure, the results of this work will give the proper direction for deposition condition changes to obtain the desired structure.

(2) The addition of excess chlorine to the system decreases deposition rate. This indicates that in the temperature range studied, the deposition of silicon is the rate-limiting step.

(3) Residual stress patterns were correlated with deposit structure. Coarsely nucleated material was found to be in tension at the first-deposited surface while finely nucleated material was in compression.

(4) The crystallographic structure of the material was studied. Since cubic and hexagonal structures are present in deposits in varying amounts, their relative amounts in relation to deposition conditions was studied. No correlation with residual stress was determined.

(5) Biaxial tensile testing of several samples of CVD SiC gave an average strength of about 82,000 psi. In relation to specimen size, this is somewhat higher than would be predicted from bend test data. It is probably a more realistic value for intrinsic strength of CVD SiC prior to machining.

REFERENCES

1. T. D. Gulden, J. Am. Ceramic Soc. 52, 585 (1969).
2. J. R. Weiss, Ph.D. Thesis, R.P.I., Troy, N.Y., May, 1974.
3. R. C. Oliver, Chem. Eng. 69, 121 (1962).
4. P. Popper and I. Mohyudin, Special Ceramics, 1964, p. 45-59.
5. A. Verma and P. Krishna, "Polymorphism and Polytypism in Crystals", 1966.
- 5A. J. M. Harris, et. al., 2nd International CVD Conference, 795 (1970) E.C.S.
6. W. F. Knippenberg, Phillips Research Reports 18, 161 (1963).
7. H. Sato, S. Shinozaki, M. Yessik, J. of App. Physics 45, 1639 (1974).
8. H. Sato, S. Shinozaki, Mat. Res. Bull. 10, 257 (1975).
9. A. C. Airey, P. J. Cartwright, and P. Popper, Special Ceramics 6, 147 (1975).
10. D. E. Lloyd and V. C. Howard, Special Ceramics 4, 103 (1968).
11. B. S. Cartwright and P. Popper, Science of Ceramics 5, 473 (1970).
12. R. L. Crane and V. J. Krukonis, Am. Ceramic Soc. Bull. 54, 184 (1975).
13. J. J. Gebhardt, R. A. Tanzilli and T. A. Harris, J. Electchem. Soc. 123, (1976).
14. R. E. Engdahl, Final Report DCI F-37, U.S. Army Res. Office DAAG29-76-C-0030.
15. T. I. Kamins, J. Electrochem. Soc. 121, 681 (1974).
16. T. P. Hoar, D. J. Arrowsmith, Trans. of Inst. of Metal Finishing 36, 1 (1958).
17. C. F. Powell, Chapter 7 in "Vapor Deposition, ed. C. F. Powell, J. H. Oxley, and J. M. Blocher, Jr., (1966).
18. A. H. Gomes De Mesquita, Acta Cryst. 23, 610 (1967).
19. R. A. Causey, et. al., J. Amer. Cer. Soc. 61, 221 (1978).
20. E. Klokholm and B. S. Berry, J. Electrochem. Soc. 115, 823 (1968).
21. F. I. Baratta, Am. Cer. Soc. Bull. 57, 806 (1978).
22. M. Y. Poperka, Phys. Metals Metallog. 20, 114 (1965).
23. R. Stevens, J. of Matls. Sci. 7, 517 (1972).

24. K. L. Chopra, "Thin Film Phenomena", (1969).
25. R. Weil, Plating 58, 137 (1971).
26. J. D. Finegan and R. W. Hoffman, Case Inst. Tech., AEC Report 18, Cleveland, Ohio (1961).
27. J. B. Wachtman, Jr., et. al., J. of Mtls. I, 188 (1972).
28. C. A. Johnson, G. E. Report, 78 CRD009 (1978).

Figure 1 Coarse vs. Fine Nucleation

100X Magnification

Both were flat plate runs: 1400 °C

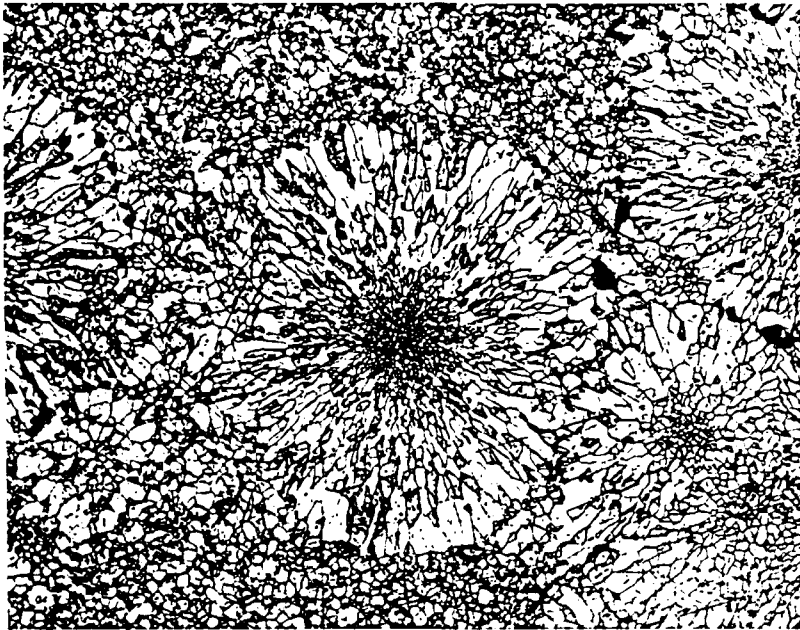
Pressure = 5mmHg

4 CFH Hydrogen

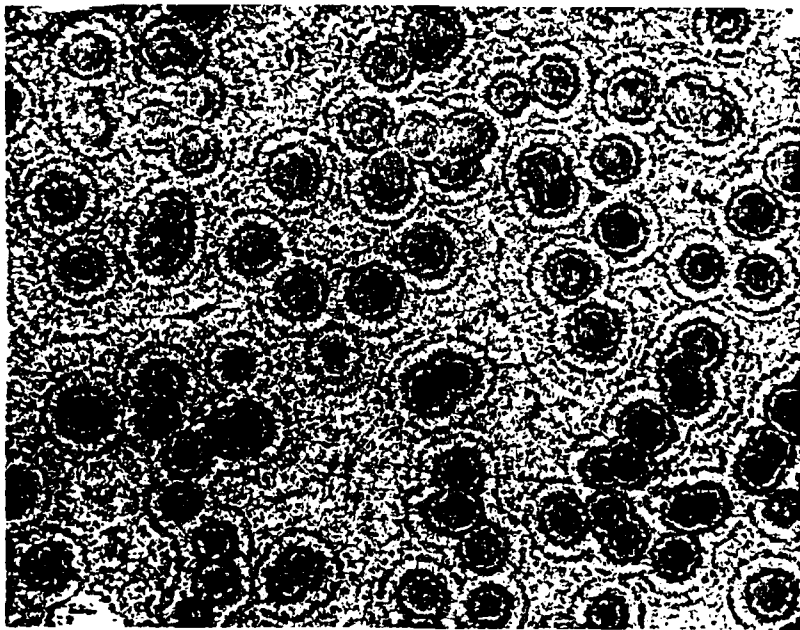
Hydrogen:MTCS=2.0

1(A) Run 2005

1(B) Run 2007



(A)



(B)

Figure 2

Decomposition of Methyltrichlorosilane

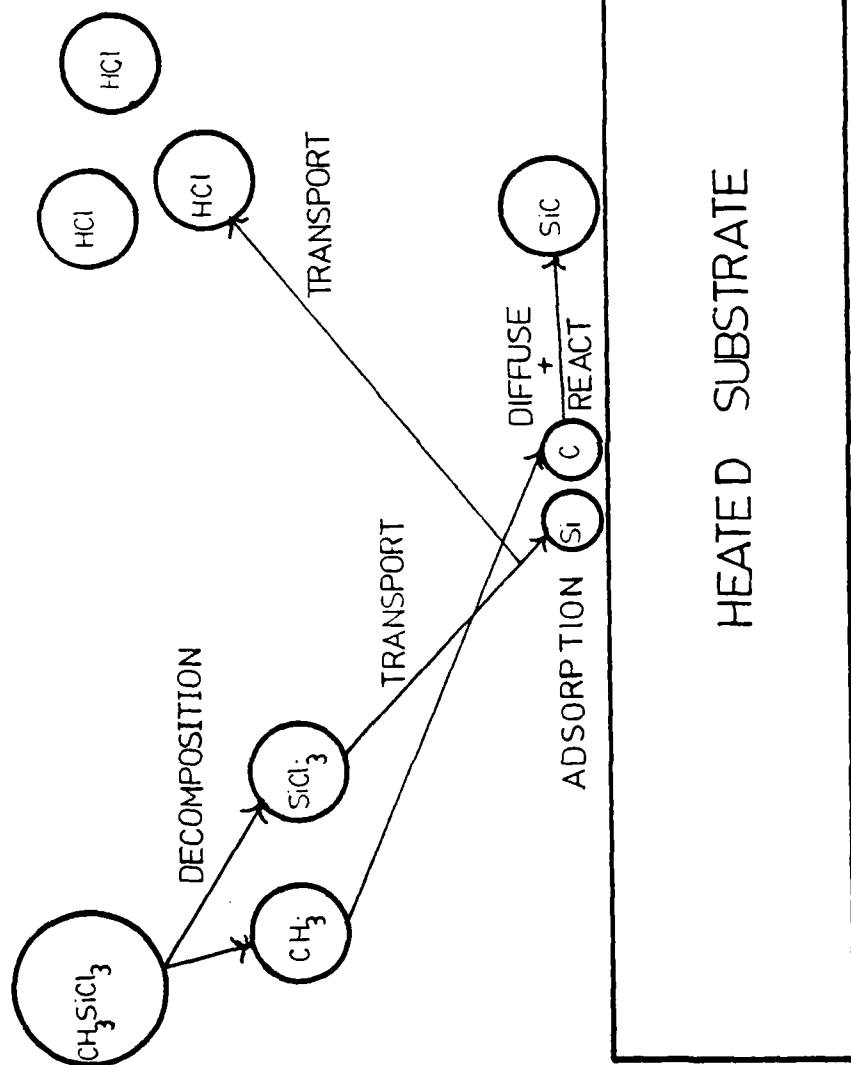


Figure 3

Decomposition of MTCS after Cartwright¹¹

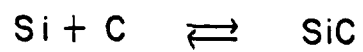
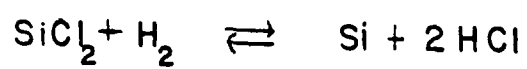
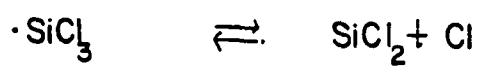
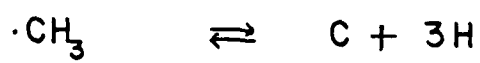
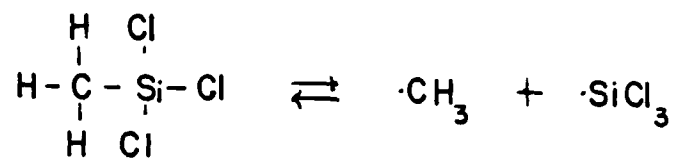


Figure 4
Schematic of Deposition Apparatus

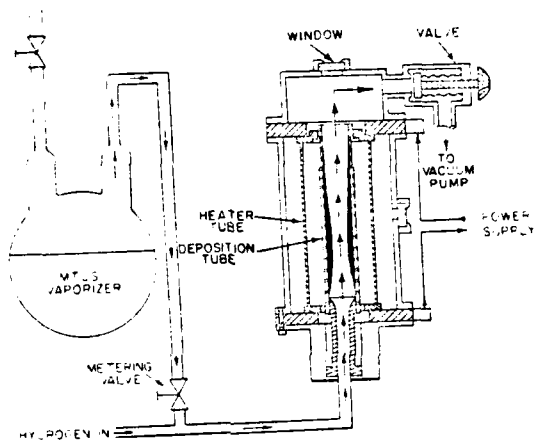
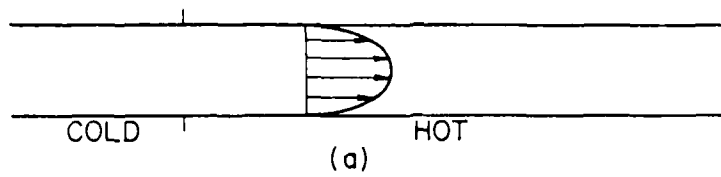
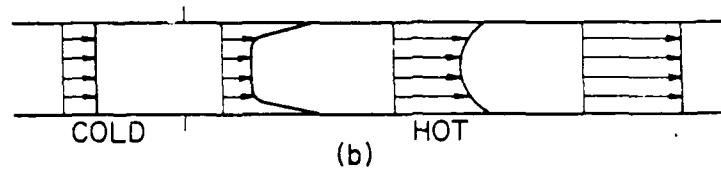


Figure 5

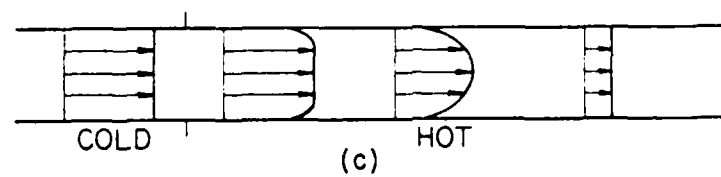
Profiles for "Hot Wall" Deposition System



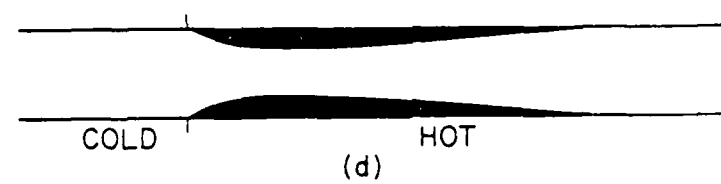
FLOW PROFILE



TEMPERATURE



CONCENTRATION



DEPOSITION

Figure 6

Deposition Profiles as a Function of Temperature

After Weiss²

DEPOSITION RATE PROFILES

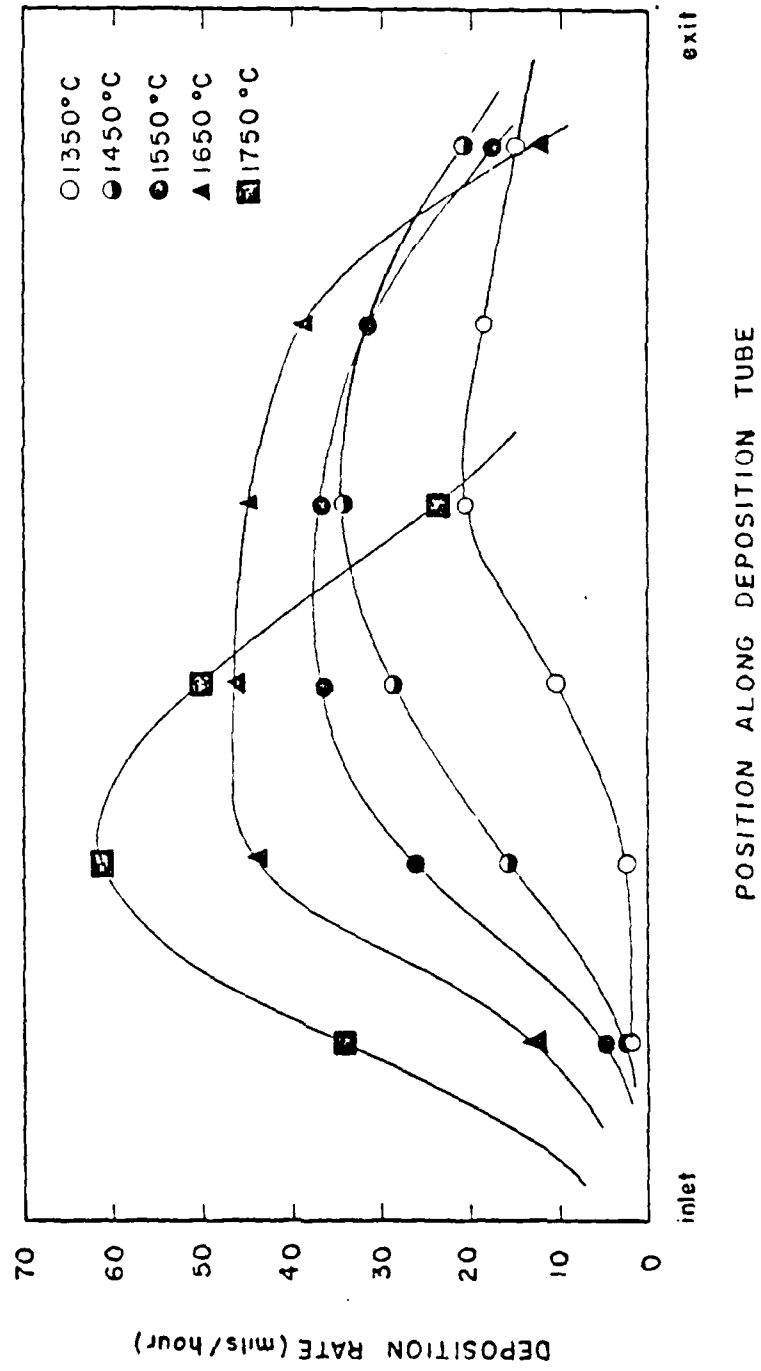


Figure 7

Deposition Profiles for Methyltrichlorosilane
vs. Methyldichlorosilane

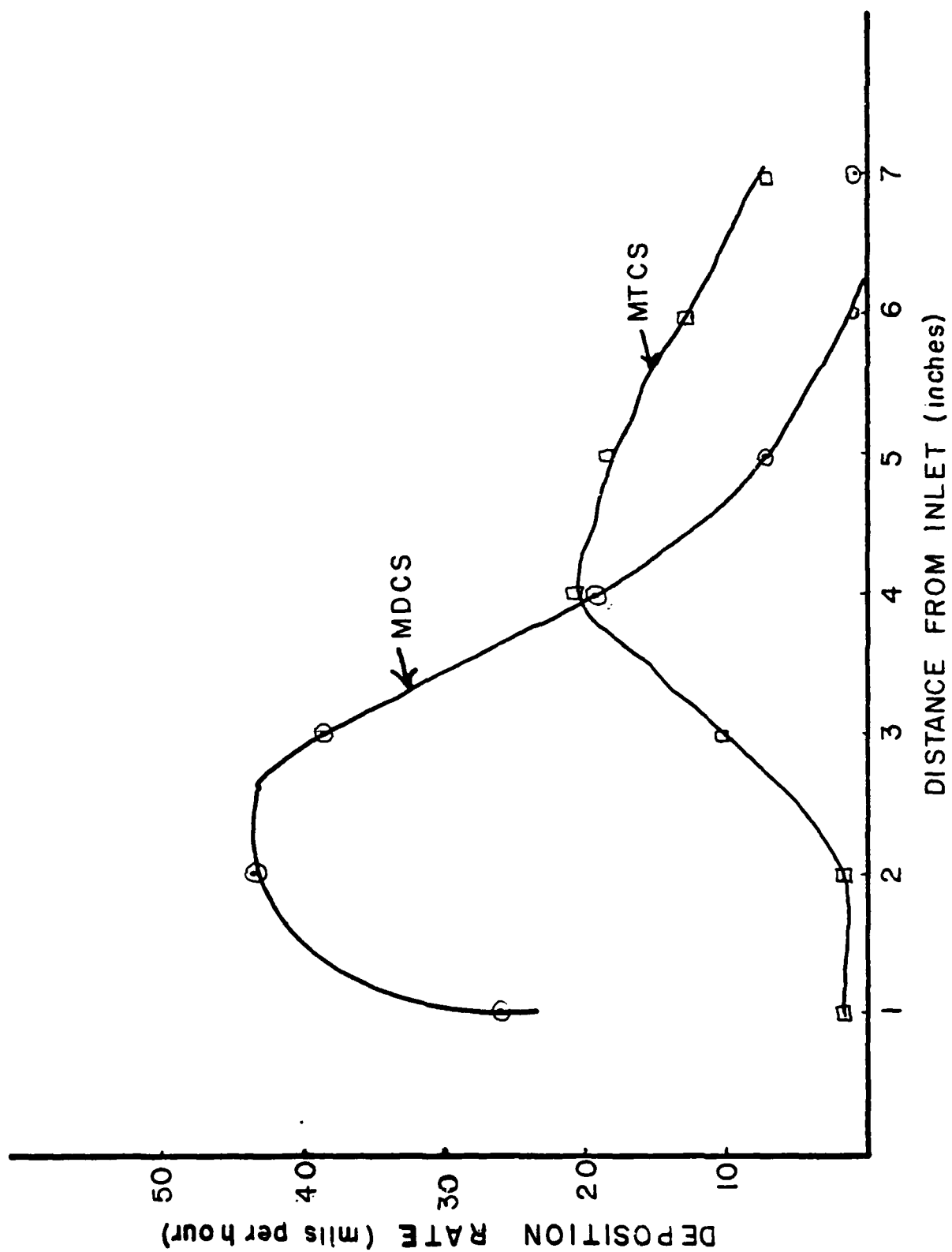


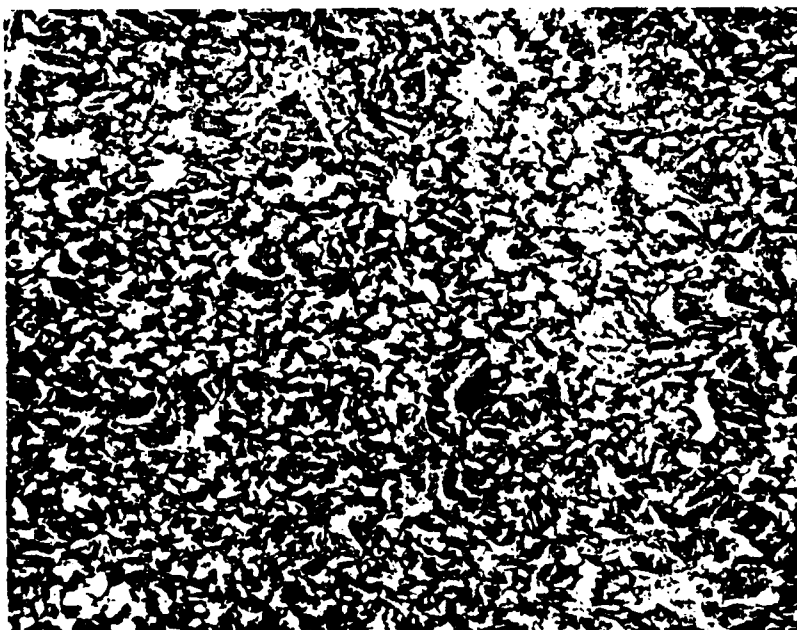
Figure 8

Effect of Temperature

Scanning Electron Micrographs 1000X



1650 °C

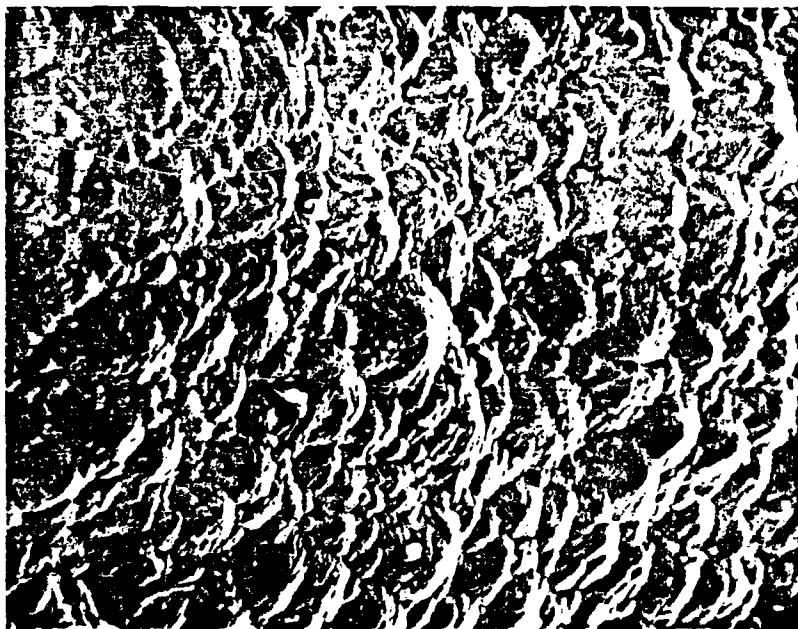


1450 °C

Figure 9

Effect of Concentration

Scanning Electron Micrographs 1000X



8:1 H₂:MTCS

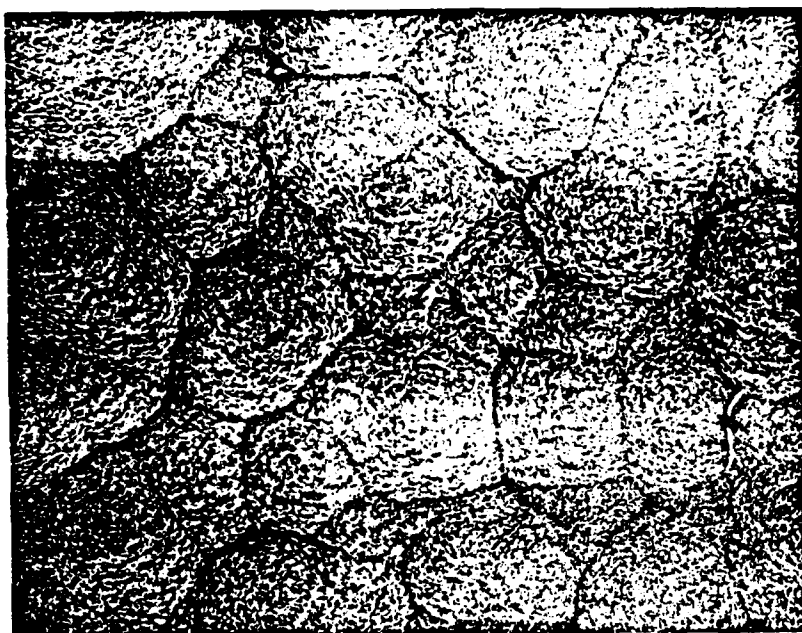


2:1 H₂:MTCS

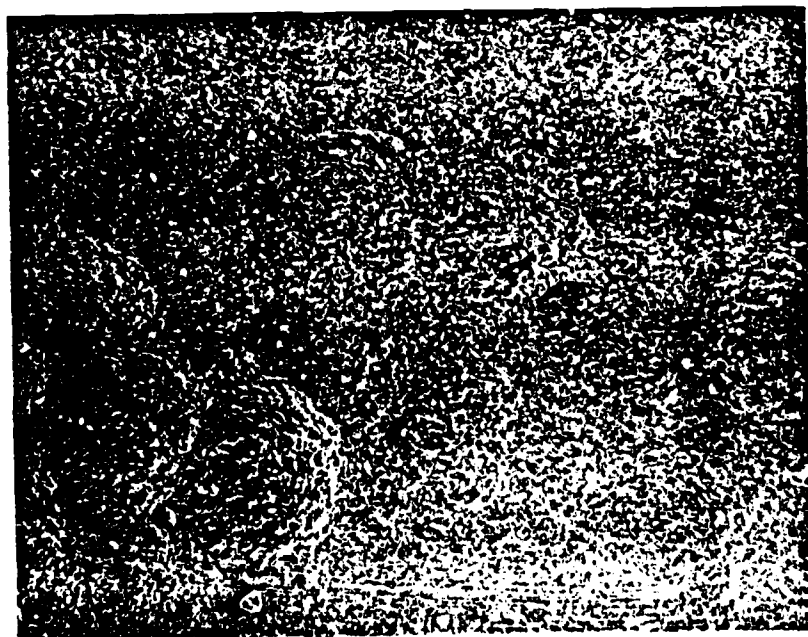
Figure 10

Effect of Pressure

Scanning Electron Micrographs 50X



20 mmHg



5 mmHg

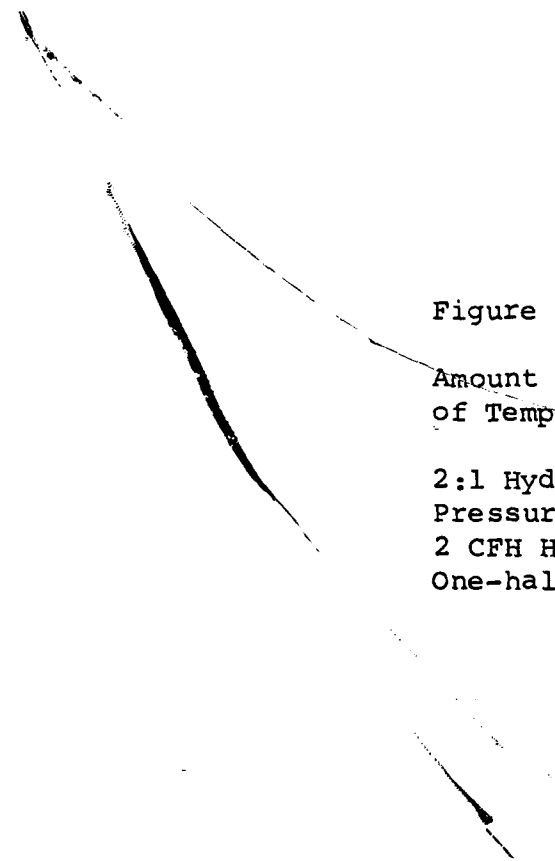


Figure 11

Amount of Non-cubic Material as a Function
of Temperature

2:1 Hydrogen to MTCS
Pressure=5mmHg
2 CFH Hydrogen
One-half inch bore tube

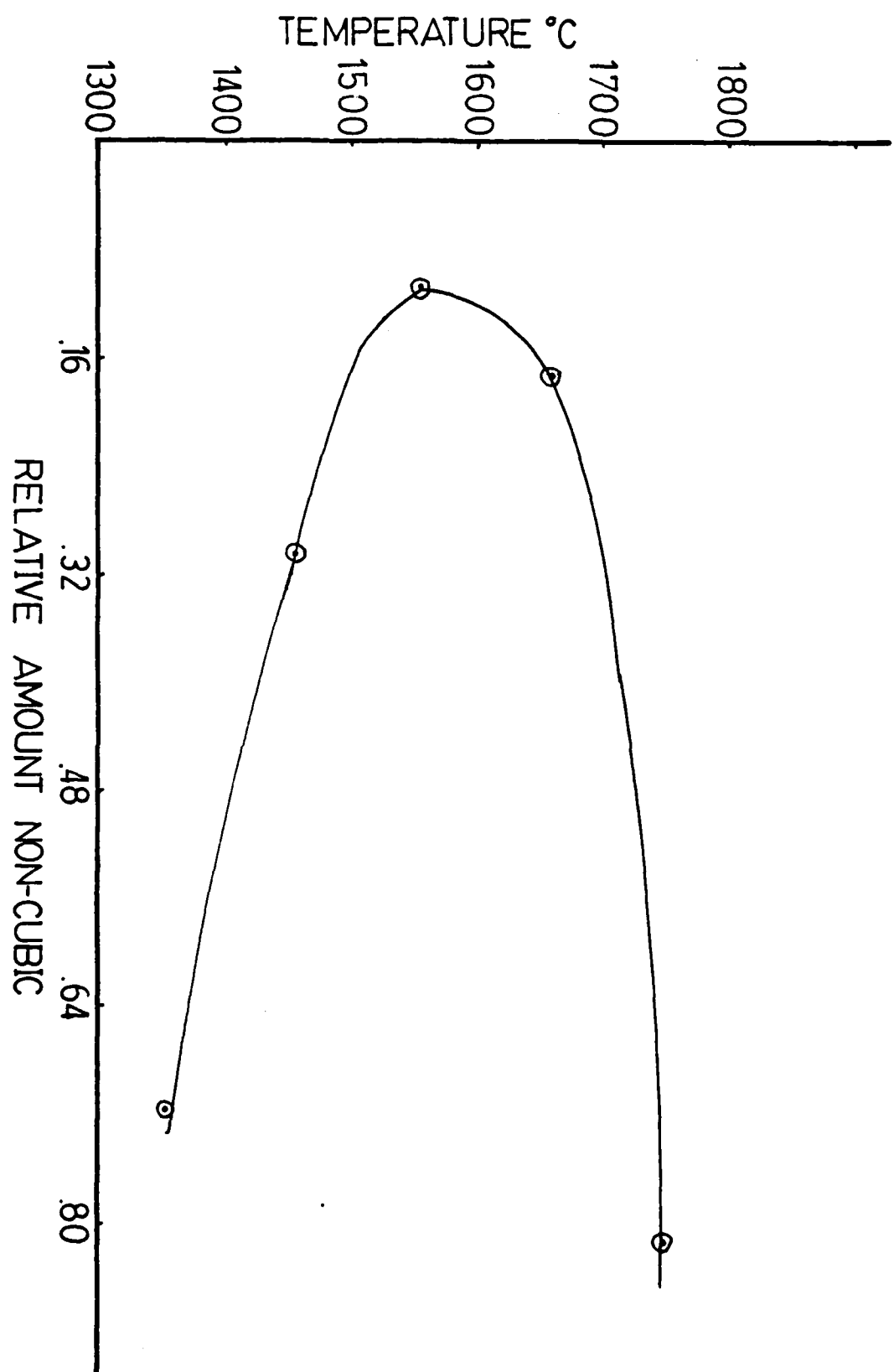


Figure 12

Defect Theory of Residual Stresses

After Hoar and Arrowsmith¹⁶

12(A) Effect of Surface Vacancies

12(B) Effect of Surface Adsorbed Atoms

GAS

SOLID

T T T T T
T T T T T
T T T T T
T T T T T

T T T T T
T T T T T
T T T T T
T T T T T

(A)

SURFACE
VACANCIES

(B)

ADSORBED
ATOMS

Figure 13

Residual Stress vs. Thickness for a Flat Plate

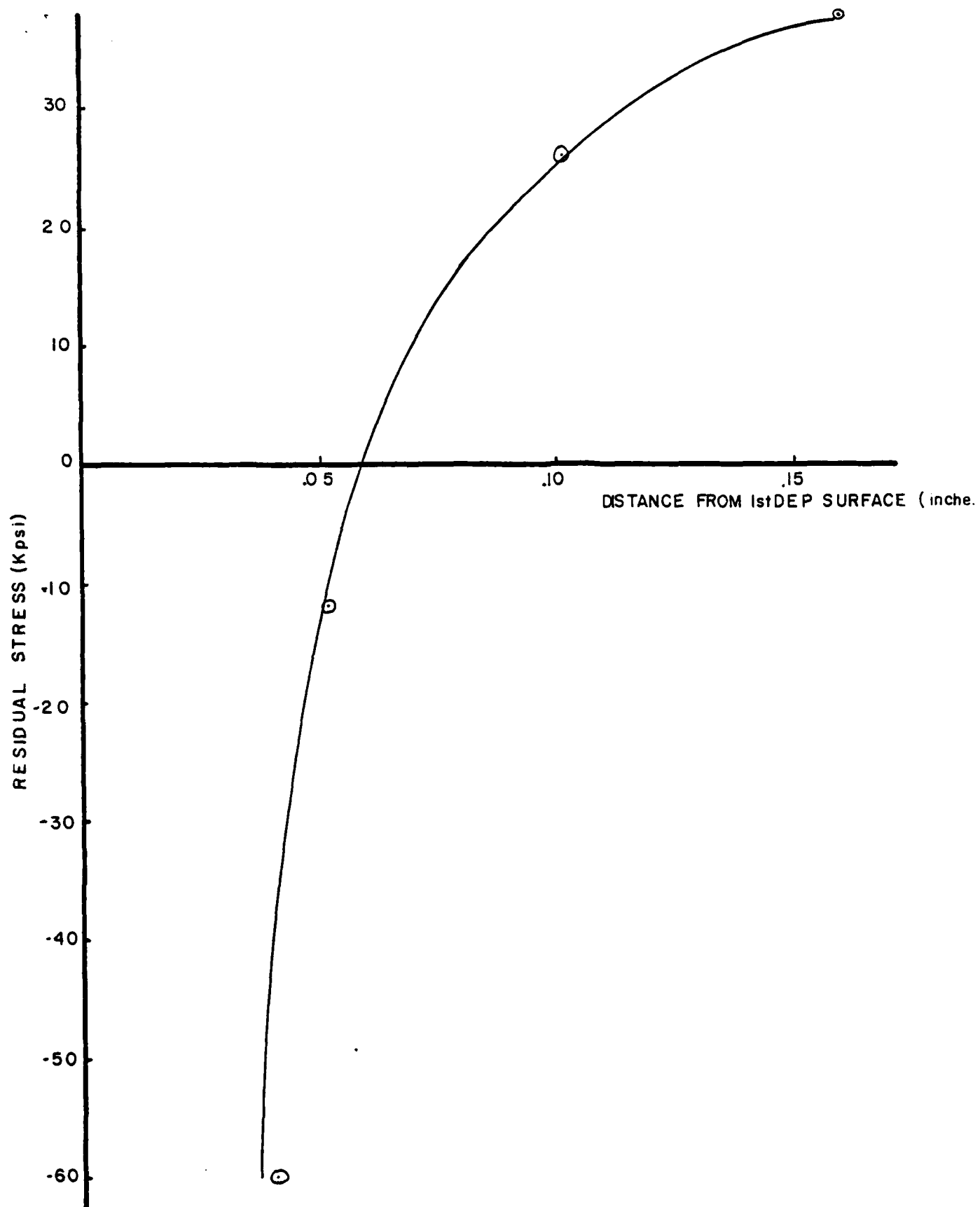
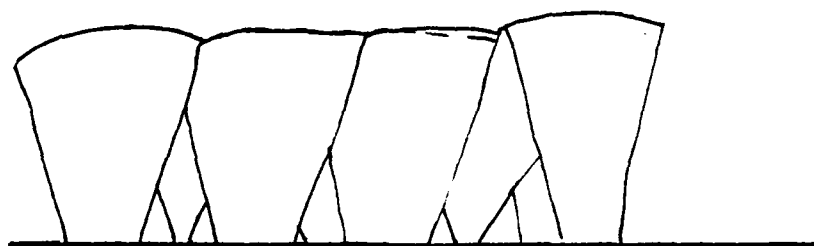


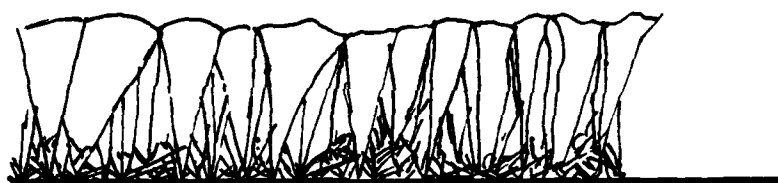
Figure 13A

(A) Coarsely Nucleated Structure.

(B) Finely Nucleated Structure.



COARSELY NUCLEATED



FINELY NUCLEATED

Figure 14

Preferred Orientation as a Function of Material
Removed from the First-Deposited Surface

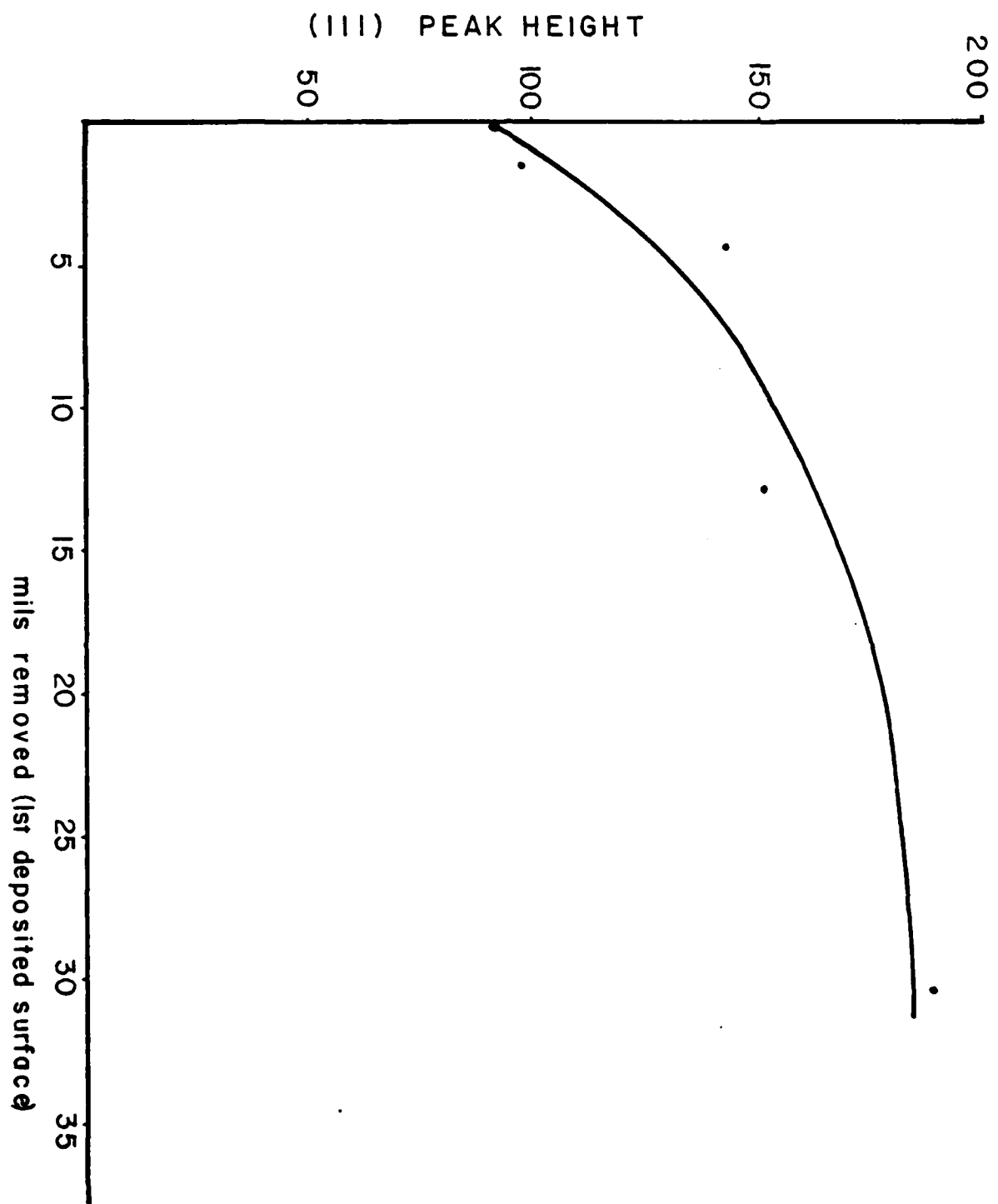


Figure 15

Sphere-like Material Found in a Poorly
Nucleated Deposit

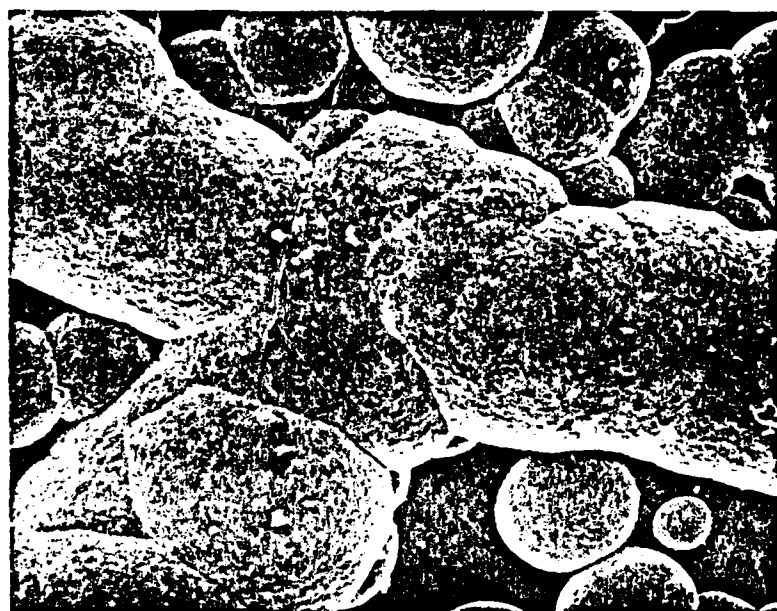
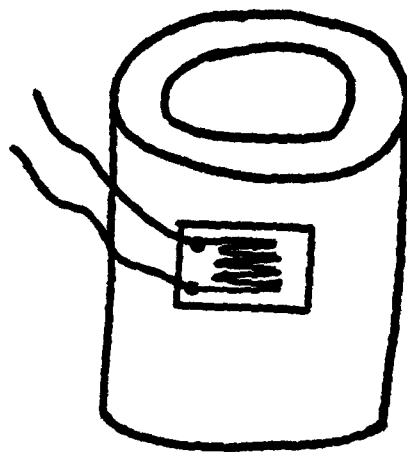


Figure 16

Measurement of strain in 1" cylinders
of material to obtain residual stress
data.

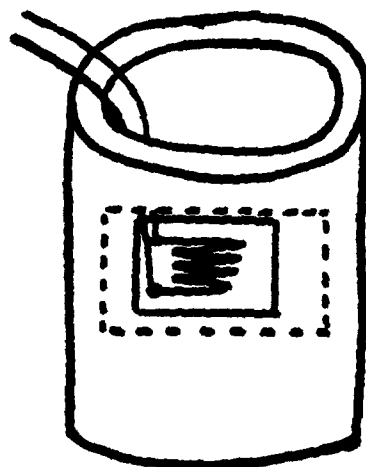
TO
AMPLIFIER



GRINDING FIRST
DEPOSITED SURFACE

A

TO
AMPLIFIER



GRINDING LAST
DEPOSITED SURFACE

B

Figure 17

Biaxial Stress Measurement Assembly.

